Constrained 3D magnetotelluric inversion with realistic prior information

Ruijin Kong[1], Zhengyong Ren[1], Jingtian Tang[1]
[1]School of Geosciences and Info-Physics, Central South University, Changsha 410083, China,
kongruijin@csu.edu.cn, renzhengyong@csu.edu.cn, jttang@csu.edu.cn

SUMMARY

The magnetotelluric (MT) method is a powerful tool for mapping subsurface electrical structures, yet it faces challenges in 3D inversion due to data limitations, resulting in ill-posed and non-unique problems. This paper introduces a novel algorithm for constrained inversion of 3D MT data, integrating structural and rock-physics constraints. Our approach employs unstructured tetrahedral meshes for subsurface discretization and utilizes the Gauss-Newton method to minimize the objective function. Structural constraints are applied using the cross-gradient method, while rock-physics constraints are incorporated through the guided fuzzy c-means clustering (GFCM) method. Initially, we validated our algorithm using a block anomaly model with undulating topography, comparing the results of unconstrained and constrained inversion. The findings demonstrate that constrained inversion produces a more accurate model. This research enhances our understanding of the Earth's subsurface by effectively integrating structural and rock-physics constraints into 3D MT inversion, offering a valuable tool for geophysical exploration and research.

Keywords: Magnetotelluric, Constrained inversion

INTRODUCTION

The magnetotelluric (MT) method is a crucial geophysical technique used to investigate the Earth's subsurface structure (Tikhonov, 1950). By analyzing electromagnetic fields measured at the surface, it provides insights into the subsurface's electrical distribution (Rikitake, 1948; Cagniard, 1953). However, 3D inversion of MT data is challenging due to data limitations and noise, leading to nonuniqueness problem (Moorkamp et al, 2011; Colombo and Rovetta, 2018).

Incorporating prior information can narrow the solution space, potentially leading to improved inversion results (Zhdanov et al, 2012; Moorkamp, 2023). In recent years, there has been a notable trend toward using joint and constrained inversions to enhance the resolution and reliability of geophysical models (Gallardo and Meju, 2003; Zhdanov et al, 2012; Franz et al, 2021). Structural constraints assume that different subsurface physical models share similar structures. Representative methods include the cross-gradient method (Gallardo and Meju, 2003), which aligns gradient directions of different models. Rock-physics constraints integrate additional geological information like parameter relationships or statistical data, exemplified by the guided fuzzy c-means (GFCM) clustering (Sun and Li, 2015), which concentrates inversion model parameters around specified centers, enhancing geological interpretation.

Despite notable research advancements in constrained inversion in recent years (Lelièvre et al, 2012; Colombo and Rovetta, 2018; Zhang et al, 2023), existing methods predominantly address 2D cases or utilize structured meshes. Few studies have explored constrained inversion techniques in the context of complex 3D models. Consequently, there is a pressing need for the development of 3D constrained inversion software equipped with crucial functionalities. Such software should use unstructured tetrahedral meshes to accommodate undulating topography and the complex geometries of 3D geological structures. Furthermore, it should effectively integrate a variety of prior information sources to enhance the accuracy and reliability of inversion

results.

This paper presents an algorithm for constrained inversion of 3D MT data using tetrahedral meshes. The algorithm integrates structural and rock-physics information through cross-gradient and GFCM constraints. By discretizing the study area with tetrahedral meshes, the algorithm effectively handles complex topography. The Gauss-Newton method is employed to minimize the objective function, ensuring convergence of the constrained inversion algorithm. We validate the algorithm with a synthetic model. The results demonstrate that our constrained inversion approach significantly enhances the reliability and resolution of the inversion model.

METHODOLOGY

In this section, we briefly introduce the theory of the constrained inversion algorithm developed in this paper. First, we present the composition of the objective function. Next, we explain the basic principles of the cross-gradient method and the GFCM method. Finally, we describe how the objective function is minimized using the Gauss-Newton method.

Objective function

We consider the constrained inverse problem as a minimization of the objective function:

$$\boldsymbol{\phi}(\mathbf{m}) = \boldsymbol{\phi}_d(\mathbf{m}) + \alpha\boldsymbol{\phi}_m(\mathbf{m}) + \beta\boldsymbol{\phi}_{\mathrm{cg}}(\mathbf{m}) + \gamma\boldsymbol{\phi}_{\mathrm{gfcm}}(\mathbf{m}), \tag{1}$$

where $\boldsymbol{\phi}_d$ and $\boldsymbol{\phi}_m$ are data misfit and model roughness term, respectively; $\boldsymbol{\phi}_{\mathrm{cg}}$ is the cross-gradient term and $\boldsymbol{\phi}_{\mathrm{gfcm}}$ is the GFCM clustering term; three factors (α, β and γ) are the trade-off parameters; $\mathbf{m}$ is a vector given by the logarithmic transformation of the electrical conductivity (Kim and Kim, 2011).

Cross-gradient method

The cross-gradient function, which measures the structural resemblance of different models, is defined as the cross product of the gradients (Gallardo and Meju, 2003):

$$\mathbf{t} = \nabla\mathbf{m}(x, y, z) \times \nabla\mathbf{m}_s(x, y, z), \tag{2}$$

where m is the conductivity model, and m_s is a fixed priori model obtained from geological or geophysical information.

Guided fuzzy c-means (GFCM) clustering

Assuming there are C types of geological units within the study area, with their respective resistivities being $t = [t_1, t_2, ..., t_C]$, we can formulate the GFCM clustering problem as follows (Sun and Li, 2015):

$$\boldsymbol{\phi}_{\mathrm{gfcm}}(\mathbf{m}) = \sum_{i=1}^{M}\sum_{j=1}^{C} u_{ij}^{q} \left\| m_i - v_j \right\|_2^2 + \sum_{j=1}^{C} \eta_j \left\| v_j - t_j \right\|_2^2, \tag{3}$$

where M is the number of model parameters; v_j is the center of the jth cluster; u_{ij} is the membership of the ith model cell with respect to the jth cluster; q is a fuzzy parameter, usually set to 2.0; and η_j is a weighting factor, which is determined according to the reliability of the prior cluster center t_j.

Finally, to ensure the convergence of the inversion algorithm, we used the Gauss-Newton method to minimize the objective function. The Gauss-Newton method is particularly advantageous due to its efficiency and robustness in handling non-linear least squares problems. For more details, please refer to Grayver et al (2013).

SYNTHETIC TEST

The synthetic model, shown in Figure 1, contains two block anomaly objects within a homogeneous half-space of 100 Ωm with undulating topography. The resistivities of the two anomalies are set to 10 Ωm and 1000 Ωm. For forward modeling, the $40 \times 60 \times 20$ km study area was discretized into 822,932 fine cells, with a total of 1,324,227 cells when including boundary cells and the air layer. The full impedance tensors of 77 sites and 16 frequencies uniformly distributed on a logarithmic scale in the frequency range of 0.001-10 Hz were generated. In addition, 5 percent Gaussian noise was added to the data.

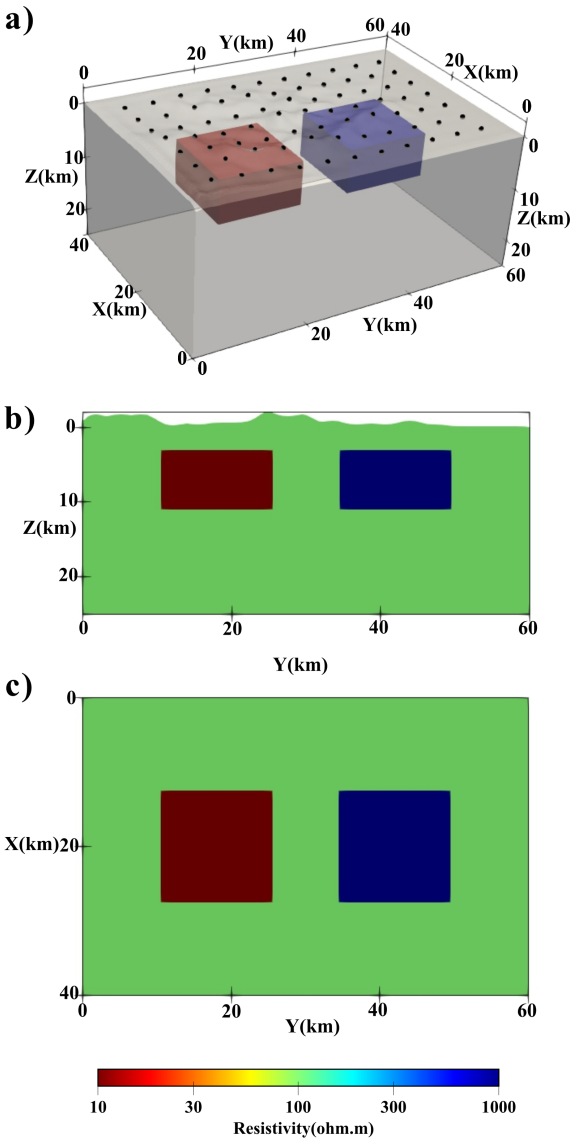

Figure 1: True model of the first synthetic example. a) 3D view, the black points at the surface represent the MT sites. b) The vertical slice at X = 20 km. c) The horizontal slice at Z = 7 km.

The vertical slices of inversion results are shown in Figure 2 to compare different constraints. True boundaries of anomalous targets are outlined in white. Compared to the real model (Figure 2a), all inversions capture the basic features of the anomalies. Unconstrained inversion (Figure 2b) recovers a resistor with resistivity around 300 Ωm and a conductor with a blurred boundary, especially the lower boundary. With the cross-gradient constraint (Figure 2c), boundaries become clearer and more consistent with the true values, indicating its effectiveness but weakness. GFCM constrained inversion yields significantly improved results (Figure 2d), with the resistor's resistivity recovered to about 800 Ωm, closer to the true value. Simultaneous application of both constraints recovers resistivity values close to the true ones and restricts targets within their true boundaries, though deeper structures are not fully recovered.

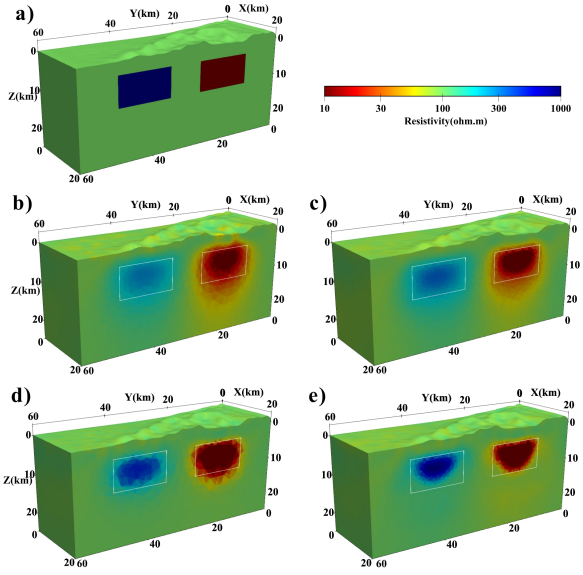

Figure 2: Inversion results of the first synthetic example at X = 20 km. a) The true resistivity model. b) Unconstrained inversion. c) Cross-gradient constrained inversion. d) GFCM constrained inversion. e) Cross-gradient and GFCM constrained inversion. The true boundaries of the anomalous targets are outlined by the white line.

CONCLUSIONS

In this study, we developed a constrained inversion algorithm for 3D MT data, integrating structural and lithological constraints. Through validation on a synthetic model, our method significantly improved the resolution and reliability of subsurface electrical structures.

ACKNOWLEDGMENTS

This work is financially supported by the National Key Research and Development Program

of China (2023YFC2906802), the National Natural Science Foundation of China (42250102, 42130810, 72088101) , the Fund from the Key Laboratory of Geophysical Electromagnetic Probing Technologies of Ministry of Natural Resources (KLGEPT202201) and the Graduate Student Innovation Program of Central South University (2023ZZTS0444). This work was supported in part by the High-Performance Computing Center of Central South University. We thank Dr. Wangqi Ren for his contribution to data processing, and Dr. Minghong Liu for his advice throughout the preparation of this paper. We also express our appreciation to Zejiang Hao for his help in the drawing process.

REFERENCES

Cagniard L (1953) Basic theory of the magnetotelluric method of geophysical prospecting. Geophysics 18:605–635

Colombo D, Rovetta D (2018) Coupling strategies in multiparameter geophysical joint inversion. Geophysical Journal International 215(2):1171–1184

Franz G, Moorkamp M, Jegen M, Berndt C, Rabbel W (2021) Comparison of different coupling methods for joint inversion of geophysical data: A case study for the namibian continental margin. Journal of Geophysical Research: Solid Earth 126(12):e2021JB022092

Gallardo LA, Meju MA (2003) Characterization of heterogeneous near-surface materials by joint 2d inversion of dc resistivity and seismic data. Geophysical Research Letters 30(13)

Grayver AV, Streich R, Ritter O (2013) Three-dimensional parallel distributed inversion of csem data using a direct forward solver. Geophysical Journal International 193(3):1432–1446

Kim HJ, Kim Y (2011) A unified transformation function for lower and upper bounding constraints on model parameters in electrical and electromagnetic inversion. Journal of Geophysics and Engineering 8(1):21–26

Lelièvre PG, Farquharson CG, Hurich CA (2012) Joint inversion of seismic traveltimes and gravity data on unstructured grids with application to mineral exploration. Geophysics 77(1):K1–K15

Moorkamp M (2023) Joint and constrained inversion as hypothesis testing tools. Applications of Data Assimilation and Inverse Problems in the Earth Sciences 5:252

Moorkamp M, Heincke B, Jegen M, Roberts AW, Hobbs RW (2011) A framework for 3-d joint inversion of mt, gravity and seismic refraction data. Geophysical Journal International 184(1):477–493

Rikitake T (1948) Notes on electromagnetic induction within the earth. Bull Earthq Res Inst 24(1):4

Sun J, Li Y (2015) Multidomain petrophysically constrained inversion and geology differentiation using guided fuzzy c-means clustering. Geophysics 80(4):ID1–ID18

Tikhonov AN (1950) On the determination of electric characteristics of deep layers of the Earth's crust. Dokl Akad Nauk SSSR 73:295–297

Zhang R, Li T, Liu C, He H, Huang X, Vatankah S (2023) Geophysical joint inversion based on mixed structural and rock-physics coupling constraints. Geophysics 88(2):K27–K37

Zhdanov MS, Gribenko A, Wilson G (2012) Generalized joint inversion of multimodal geophysical data using gramian constraints. Geophysical Research Letters 39(9)